Original Research

The inhibitory effect of iridoid glycoside extracted from *Fructus Gardeniae* on intracellular acidification and extracellular Ca^{2+} influx induced by influenza A virus

Shanshan Guo, Yingjie Gao, Yahong Jin, Xuechuan Tian and Xiaolan Cui

Institute of Chinese Materia Medica, China Academy of Chinese Medical Sciences, Chaoyang District, Beijing 100029, China
Corresponding author: Cui Xiaolan. Email: cuixi2812@sina.com

Abstract

Influenza is a serious public health problem that causes severe illnesses and deaths for higher risk populations. Iridoid glycoside is one of the main active components from *Fructus Gardeniae* with antivirus and anti-inflammatory characteristics. The present study was designed to investigate the inhibitory effect of iridoid glycoside extracted from *Fructus Gardeniae* (IGE) on influenza and explore the potential mechanism of the action. *In vitro*, IGE exhibited highest activity against influenza virus A/FM1/47 induced visible cytopathic effect (CPE), with half maximal inhibitory concentration and therapeutic index values of 3.15 mg/mL and 11.37, respectively, and the replication of influenza virus A/FM1/47 was inhibited markedly by IGE at the concentrations of 25, 12.5 and 6.25 mg/mL. *In vivo*, treatment of mice with IGE decreased pulmonary index, viral titers and M2 protein expression in a dose-dependent manner. IGE increased the declining pHi induced by influenza virus significantly at the concentrations of 25 and 12.5 mg/mL 0.5 or 1 h post-infection, respectively. IGE treatment inhibited elevation of $[Ca^{2+}]i$ significantly at the concentrations of 25 and 12.5 mg/mL 0.5, 1 or 24 h post-infection, respectively. In addition, IGE reduced the rate of early-apoptotic cells at the concentrations of 25, 12.5 and 6.25 mg/mL, but showed no apparent effect on the rate of late-apoptotic cells. Our study demonstrates that IGE possesses antiviral activity against influenza A virus, and the antiviral action might be related to the inhibition of intracellular acidification and Ca^{2+} influx during fusion and uncoating of influenza replication cycle.

Keywords: Iridoid glycoside, *Fructus Gardeniae*, influenza A virus, pHi, Ca^{2+} influx

***Experimental Biology and Medicine* 2014; 239: 986–997. DOI: 10.1177/1535370214530361**

Introduction

Influenza viruses are enveloped, negative-strand RNA viruses and include A, B, and C types.[1] Influenza A viruses cause significant morbidity and mortality in humans, mammals and birds through epidemics or pandemics, sometimes with devastating consequences.[2,3] For instance, it was estimated that Spanish influenza in 1918 infected one-third of the world's population and killed 50 million people worldwide,[4–6] and outbreaks of the highly pathogenic avian H5N1 influenza A virus caused high rates of death among infants and young children in southeast Asia.[7,8] Furthermore, the emergence of a new swine-origin H1N1 influenza virus strain in 2009 posed a challenge to public health[9] and the subsequent global outbreak claimed the lives of more than 18,000.[10] Recently a novel avian influenza A virus of the H7N9 subtype has infected 126 and killed 24 people in China as of 29 April 2013, and the mortality rate has reached 20%.[11,12]

The M2 integral membrane protein of the influenza A virus is abundantly expressed at the surface of virus-infected cells *in vitro* and in the ciliated cells from lungs of mice inoculated with virus *in vivo*.[13] The function of M2 protein has been proved to be the proton channel activity that is essential for mediating endosomal acidification and RNP-M1 protein dissociation during the membrane fusion and uncoating process of influenza virus replication.[14,15] The M2 protein was also shown to be largely responsible for the 0.3–0.4 unit reduction in intracellular pH of virus-infected cells labeled with fluorescent probe SNARF-1.[16] However, amantadine affects M2 activity by plugging the M2 channel and preventing proton flow.[17]

Calcium ion homeostasis is essential for cell survival, and sustained overload of Ca^{2+} in the cytoplasm ($[Ca^{2+}]i$) will trigger programmed cell death involving apoptosis.[18,19] It was reported that disruption of Ca^{2+} homeostasis plays a pivotal role in apoptosis induced by several kinds of viral infections, including those with human T-cell leukemia

virus type 1, hepatitis C virus and human immunodeficiency virus (HIV).[20–22] In addition, the highly pathogenic H5N1 A influenza virus induced apoptosis of alveolar epithelial cells or vascular endothelial cells through extracellular Ca^{2+} influx, which is critical for the development of acute respiratory distress in humans and in mice.[23,24]

In recent years, pharmaceutical researchers have focused on screening compounds with anti-influenza virus activity from plant and traditional Chinese medicine (TCM).[25,26] *Fructus Gardeniae* has generally been used as a herbal medicine for centuries in several Asian counties for the treatment of hepatic, inflammatory and acute febrile diseases.[27–29] Gardenia extracts have been shown to possess the virus inhibitory activity against herpes simplex virus type 1, and parainfluenza virus type 1, and the principle bioactive components in the extracts are iridoid glucosides.[30,31] Indeed, a recent study has demonstrated that iridoid glucosides extracted from *Fructus Gardeniae* have anti-influenza virus activity *in vivo* and *in vitro*,[32,33] but the underlying mechanism has not yet been deciphered.

In the present study, we first evaluated the antiviral activity of iridoid glucoside extracted from *Fructus Gardeniae* against several stains of influenza A virus (including subtype H1N1 and H3N2) *in vitro* and *in vivo*. Then we investigated the inhibitory effect of IGE on M2 protein expression in the lung tissues of ICR mice and intracellular acidification mediated by M2 proton channel activity in MDCK cells infected by influenza A virus. In addition, laser scanning confocal microscopy and flow cytometry were applied to determine its effect on extracellular Ca^{2+} influx and apoptosis in MDCK cells inoculated with influenza virus.

Materials and methods

Preparation of extract sample

The sample of iridoid glucosides extracted from *Fructus Gardeniae* was provided by Professor Chenggang Huang, principle investigator at Shanghai Institute of Materia Medica, Chinese Academy of Sciences. The extract was prepared according to the method of their previous study.[34] First the powder of dried fruits (2 kg) was extracted with water and then deposited in ethanol. Then the supernatant fluid was vacuum dried and was successively fractionated into *n*-butanol fractions. Following that, the chloroform–methanol (15:1, v/v) elution fraction was separated and dried as the extract sample. The sample was stored at 4°C and dissolved in double distilled water until time of use. Eventually 10 iridoid glycosides were identified in the extract by reverse-phase HPLC (Agilent-1100 HPLC system, Agilent), UV spectrum and MS/MS spectra (G6310 ion-trap mass spectrometer, Agilent Technologies).

Animals

Male and female ICR mice (13–15 g) were obtained from Vital River Laboratory Animal Technology Co., Ltd in Beijing, China (Certificate No.SCXK 2006-0009) and maintained in an environmentally controlled breeding room (temperature: 20 ± 2°C, humidity: 50 ± 10%). The study was carried out in accordance with the rules of European Community Guidelines for care and use of animals.

Viruses and cells

Influenza A virus (H1N1) strain FM/1/47 and PR/8/34 were obtained from the National Institute for Viral Disease Control and Prevention, Chinese Center for Disease Control and Prevention. Influenza A virus strain Brisbane/59/2007(H1N1) and Brisbane10/2007(H3N2) were purchased from American Type Culture Collection (ATCC). The four strains of influenza virus were propagated in 10-day-old embryonated specific-pathogen-free chicken eggs (Merial Vital Laboratory Animal Technology Co., Ltd, Beijing, China) at 35°C and stored at −80°C. The virus titers of the four strains were determined to be $10^{-4.5}$, 10^{-4}, $10^{-3.5}$ and 10^{-2}, respectively, according to the Reed-Muench method,[35] expressed as the median tissue culture infective dose ($TCID_{50}$).

MDCK cells were obtained from the Cell Center, Institute of Basic Medical Sciences, Peking Union Medical College (Beijing, China) and grown in Dulbecco's modified Eagle's medium (DMEM) (4.5 g/L glucose, 10% fetal bovine serum [FBS], 1% penicillin/streptomycin, 2 mmol/L L-glutamine, 0.25 mol/L 2-[4-(2-hydroxyethyl)piperazin-1-yl]ethanesulfonic acid [HEPES] [all from Gibco]).

MTT cell viability assay

The effect of IGE on MDCK cell viability was determined by the MTT colorimetric assay.[36] The cells were seeded onto a 96-well plate at a concentration of 4×10^5 cells/mL and a volume of 100 μL per well. Next, 100 μL/well of various concentrations (800, 400, 200, 100, 50, 25, 12.5 mg/mL) of IGE were applied to culture wells, and the plates were incubated at 37°C and 5% CO_2 for 48 h. Then 10 μL of MTT (5 mg/mL in PBS) was added to each well and incubated for 4 h. Then the supernatant was discarded and 100 μL of dimethyl sulfoxide (DMSO) was added to each well. After the dissolution of formazan, the plates were read on a microplate reader (Thermo, VarioskanFlash) at 570 nm and 630 nm. Results obtained of cell viability for treated cells were expressed as the percentage of that in control cells (100%). The maximal non-cytotoxic concentration (TC_0) and median cytotoxic concentration (TC_{50}) were calculated from the dose response curve.

Antiviral assay

In-vitro experiments. MDCK cells were cultured in 96-well plates, exposed to different strains of influenza viruses ($100TCID_{50}$, 100 μL/well) for 1 h. Then the infected cells were incubated for 48 h with different dilutions of IGE, and the final concentrations were 25, 12.5, 6.25 and 3 mg/mL. Ribavirin was used as a positive drug control, and the final concentrations were 2.5, 1.25, 0.63 and 0.32 mg/mL. The infected cells showed obvious cytopathic effect (CPE), characterized by rounding and sloughing. Values for half maximal inhibitory concentration (IC_{50}) and therapeutic index (TI) were calculated according to

the Reed-Muench method. The experiments were carried out under biosafety level 2 conditions.

The virus replication of influenza virus strain A/FM/1/47 in MDCK cells was further detected by real time RT-PCR. Total cellular RNA was isolated by Trizol reagent (Invitrogen, USA) according to the manufacturer's instructions. RT-PCR assay was performed using the one step SYBR primescript RT-PCR kit (Takara, Japan) according to the manufacturer protocol (for primer sequences, influenza virus A/FM/1/47 matrix protein genes, forward primer 5′-ATCATTGGGATCTTGCACTT-3′ and reverse primer 5′-TCATAGACTCTGGCACTCCTT-3′, GAPDH, forward primer 5′-CCCACTCCTCCACCTTTGACG-3′ and reverse primer 5′-CACCACCCTGTTGCTGTAGCCA-3′). Influenza virus A/FM/1/47 and GAPDH transcript levels were determined by the$\Delta\Delta$CT method. The inhibition percentage was calculated as follows: % inhibition = 1− (average of IGE-treated cells infected by virus)/(average of infection control cells).

In-vivo experiments. ICR mice (13–15 g) were randomly divided into six groups with 10 mice per group (half male and half female). The groups were assigned as normal control group, infection control group and four treatment groups (three IGE treatment groups and one positive drug-amantadine treatment group). All mice except those in the normal control group were infected intranasally with 40 μL of the influenza virus strain A/FM/1/47 solution at a concentration 15 times that of the $TCID_{50}$. In the treatment groups, the inoculated mice were successively given IGE orally at a dose of 80, 40 or 20 mg/kg, or treated with amantadine hydrochloride granules (Zizhu, Beijing, China) at a dose of 55 mg/kg daily for 4 days beginning from the day of infection. Each mouse of the control group was given an equal volume of distilled water. On day 5, all the mice were sacrificed, and the body weight (BW) and lung weight (LW) were measured to calculate the pulmonary index (PI) and inhibitory rate of pulmonary indices (IRPI): PI = [LW(g)/BW(g)] × 100, IRPI = [(LW of infection control group − LW of treatment group)/(LW of infection control group–LW of normal control group)] × 100. Then the whole protein in each lung tissue was extracted and subjected to Western blot analysis.

In addition, the lung virus titers were detected by plaque assay on MDCK cells. The protein concentrations in homogenates of lungs were measured by the bicinchoninic acid (BCA) assay. The homogenates of lungs were frozen and thawed twice to release the virus. Ninety-six-well plates were seeded with 5×10^5 MDCK cells/mL, and 24 h later the serum-containing medium was removed. Homogenates were then 10-fold serially diluted and mixed with MDCK cells. After 48 h, the number of plaques was counted under a microscope. The virus titers were shown as negative lg 50% tissue culture infectious dose ($-lgTCID_{50}$).

Western blotting measurement of M2 expression

Protein extracts (20 μg) were separated by 12% SDS-polyacrylamide gel electrophoresis and transferred onto nitrocellulose membranes. The membranes were blocked at room temperature with 5%(w/v) nonfat dry milk in Tris-buffered saline/Tween (TBST) for 1 h and then incubated with primary antibody of M2 protein in a 1:500 dilution (Abcam, UK) overnight at 4°C. Blots were washed three times in TBST buffer for 5 min and incubated for 2 h with horseradish peroxidase-conjugated anti-mouse IgG secondary antibody in a 1:5000 dilution (Jackson Immunoresearch, USA). The blots were revealed by using the ECL (advanced chemiluminescence) kit (GE healthcare, UK). Densitometric measurements were performed by quantifying the density of the bands using TotalLab Quant software (TotalLab, UK).

Fluorescence staining and confocal analysis of pHi and $[Ca^{2+}]i$

MDCK cells were seeded on 35 mm glass bottom culture dishes (MatTek, USA) at a concentration of 5×10^5 cells/mL. When they grew to 80–90% confluence, both IGE (25, 12.5, 6.25 mg/mL) and influenza virus A/FM1/47 solution ($100TCID_{50}$) were concomitantly added to the cultures. After an incubation at 37°C for 0, 0.5, 1 or 1.5 h, the cells were loaded with 10 μg/mL of SNARF-1 probe (Invitrogen) for 30 min to measure the pHi. In addition, after 0, 0.5, 1, 1.5 and 24 h of infection, the cells were loaded with 10 μg/mL of fluo-3/AM probe (Invitrogen) for 30 min to detect the Ca^{2+} influx. The cells were imaged immediately with a confocal microscope (Olympus, FV1000, Japan). For SNARF-1-treated samples, we used an argon laser to excite the samples with a 488 nm wavelength and examined the emissions at 580 and 640 nm. The intensity of emission was measured using the Image-Pro Plus software (Media Cybernetics) and the ratio of 640 nm/580 nm was calculated.[37] For the measurement of intracellular calcium concentration, the samples were excited by argon laser at 488 nm, and the intensity of emission was detected at the 530 nm wavelength.[38]

Measurement of apoptosis

MDCK cells were planted on six-well plates (Corning) to near confluence and subjected to FM1 solution for 1 h as described above. Then the infected cells received treatments as indicated in confocal analysis. After 24 h of culture at 37°C, 200 μL of cells (1×10^6 cells) were labeled fluorescently for detection of apoptotic and necrotic cells by adding 200 μL of binding buffer and 10 μL of Annexin V-FITC (Biosea Biotechnology, Beijing, China) to each sample. Samples were mixed gently and incubated at room temperature in the dark for 15 min. Just before analysis by flow cytometry (BD FACSAria, USA) using 488 nm excitation, 5 μL of PI (Biosea Biotechnology) were added to each sample. A minimum of 10,000 cells within the gated region were analyzed.

Statistics

All data are presented as mean ± standard error of the mean (SEM). Results were analyzed by one-way analysis of variance (ANOVA), and significant differences were determined by the Bonferroni Test. P values ≤ 0.05 were taken as statistically significant.

Results

Effect of IGE on MDCK cells viability

Following a 48 h treatment, the effect of IGE on the viability of MDCK cells is shown in Figure 1. The concentrations ranging from 50 to 800 mg/mL had a toxic effect on MDCK cells, and the values of TC_0 and TC_{50} were calculated to be 25 and 35.82 mg/mL, respectively. In the next antiviral experiment *in vitro*, the anti-influenza activity of IGE was determined at the concentrations range from 25 to 3 mg/mL by serial two-fold dilutions.

Antiviral activities *in vitro*

As shown in Table 1, IGE possessed anti-influenza activities against the four strains of H1N1 and H3N2 subtype, and IGE exhibited highest activity against influenza virus A/FM1/47 induced visible CPE (Figure 2), with IC_{50} and TI values of 3.15 mg/mL and 11.37, respectively. The positive control drug, ribavirin, showed significant activities against all the four strains of influenza A virus at the concentrations of 2.5, 1.25, 0.63 and 0.32 mg/mL and especially exhibited highest activity against the strains of FM1 and Brisbane59.

As shown in Figure 2(e), IGE inhibited replication of influenza virus A/FM1/47 in MDCK cells in a dose-dependent manner according to the RT-PCR assay, and the percentages of inhibition were 67.11%, 59.85% and 45.41% at the concentrations of 25, 12.5 and 6.25 mg/mL respectively.

Anti-influenza virus activity *in vivo*

In the current study, the antiviral activity against influenza *in vivo* was measured using PI, IRPI and virus titers in lungs. As shown in Table 2, mice from the infection control group presented an increase in PI (1.15 ± 0.05) compared to the normal control group (0.79 ± 0.07). After 4-day's treatment, there was an obvious decrease of PI in all three IGE groups compared with the infection control group. In addition, IGE exhibited PI inhibitory activity in a dose-dependent manner (67.33%, 41.29% and 22.13%, at the concentrations of 80, 40 and 20 mg/kg, respectively). As shown in Table 3, virus titers in the lungs of mice infected by influenza virus were significantly decreased by IGE at the doses of 80, 40 and 20 mg/kg 4 days post-infection.

Inhibitory effect of IGE on influenza A virus M2 channel protein

The M2 protein has been the main target in the search for drugs against influenza A virus. Amantadine, which targets the M2 channel, is one commonly used anti-influenza virus drug.[39] To investigate whether IGE showed anti-influenza activity by inhibiting the M2 channel protein, first we used Western blotting to detect M2 expression in the lung tissues of mice infected by influenza A virus through the

Table 1 Anti-influenza virus activity of IGE *in vitro*

		Influenza virus strain			
Drug	**Index**	**FM1**	**PR8**	**Brisbane59**	**Brisbane10**
IGE	IC_{50}	3.15	8.89	6.29	4.46
	TI	11.37	4.03	5.69	8.03
Ribavirin	IC_{50}	0.22	0.32	0.22	0.45
	TI	16.14	11.09	16.14	7.89

The anti-virus activities of IGE and ribavirin against different strains of influenza were expressed as the value of IC_{50} and TI.

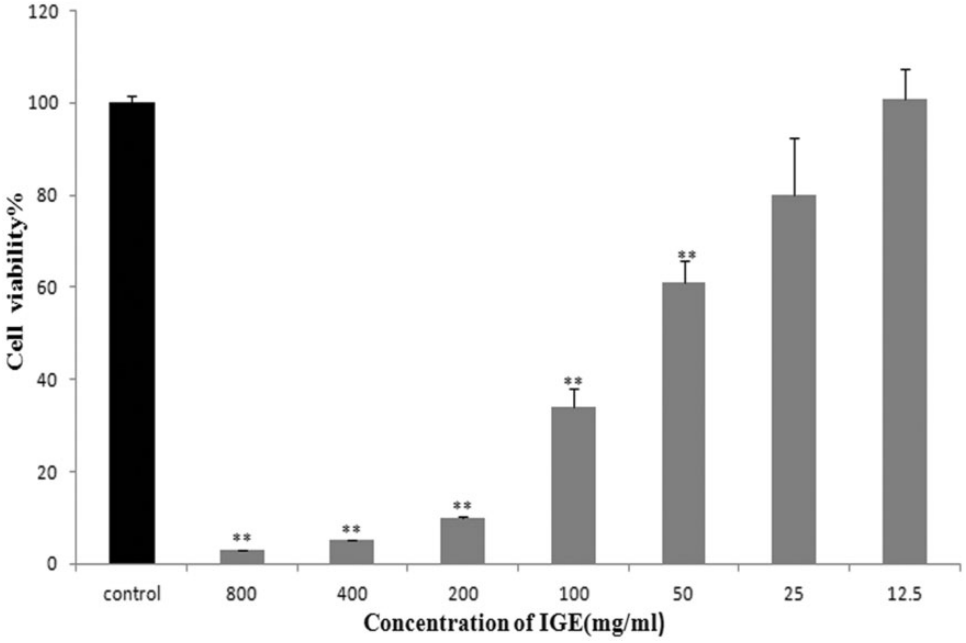

Figure 1 Cell viability of MDCK cells treated with IGE measured by MTT assay. Each value were represented as mean ± SEM, $n = 4$ independent experiment, $^{**}P < 0.01$ versus control group

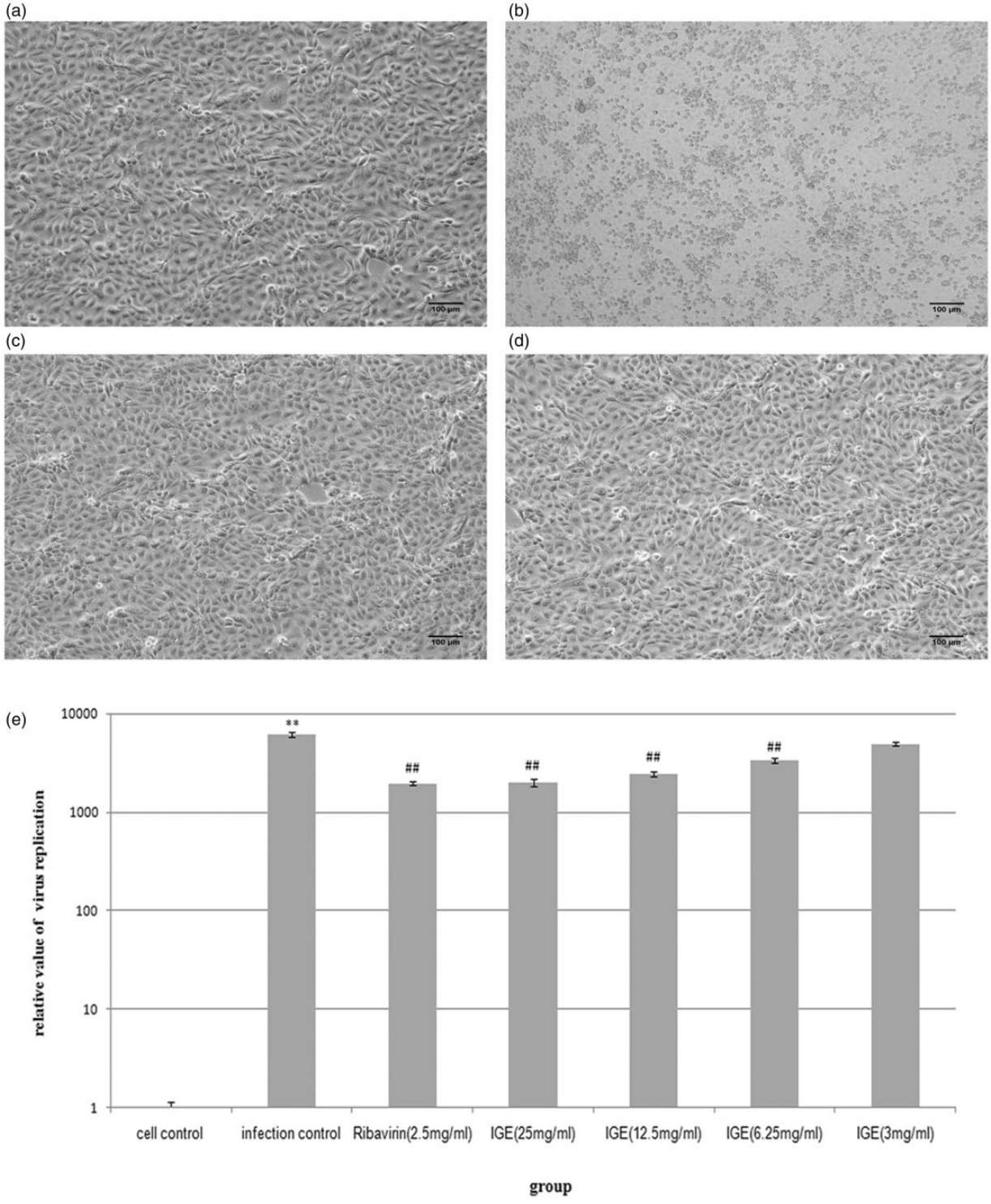

Figure 2 Antiviral activity of IGE in Madin–Darby canine kidney (MDCK) cells infected with influenza virus. (a)-(d) Cytopathic effect (CPE) observed in MDCK cells. (a) normal control group, (b) infected control group after infection 48 h, (c) IGE (25 mg/mL) treated group after infection 48 h,(d) IGE (12.5 mg/mL) treated group after infection 48 h. Typical CPE of cell rounding and crimple were observed in (b), but significantly alleviated in (c) and (d). (e) The inhibition effect of IGE on influenza virus replication in MDCK cells by RT-PCR assay. Relative values of influenza virus replication were expressed as the mean ± SEM ($n = 4$). $^{**}P < 0.01$, $^{\#\#}P < 0.05$ compared to infection control group

respiratory tract. As shown in Figure 3(a, b), in the lung tissues of normal mice, M2 expression could not be detected by Western blotting. By contrast, at day 5 post-infection with influenza A virus, M2 protein expression was strongly detected in mice lungs. The protein levels of M2 were reduced by 62.23%, 49.95% and 31.29%, respectively in the case of IGE (80, 40, 20 mg/kg) treatment as compared to the infection control. These results demonstrate that the M2

Table 2 Anti-influenza virus activity of IGE in mice

Group	PI	IRPI (%)
Normal control	0.79 ± 0.02	–
Infection control	$1.15 \pm 0.02^{**}$	–
Amantadine (55 mg/kg)	$0.89 \pm 0.03^{\#\#}$	72.62
IGE (80 mg/kg)	$0.91 \pm 0.03^{\#\#}$	67.33
IGE (40 mg/kg)	$1.00 \pm 0.03^{\#\#}$	41.29
IGE (20 mg/kg)	$1.07 \pm 0.02^{\#}$	22.13

Each group represented the value of PI and IRPI. PI was expressed as mean ± SEM ($n = 10$).
$^{**}P < 0.01$ compared to normal control group.
$^{\#\#}P < 0.01$, $^{\#}P < 0.05$ compared to infection control group.

Table 3 Inhibition effect of IGE on virus titers in lungs of mice

Group	Virus titers ($-$lgTCID$_{50}$/0.2 mL)
Normal control	0.00 ± 0.00
Infection control	$5.46 \pm 0.08^{**}$
Amantadine (55 mg/kg)	$4.17 \pm 0.18^{\#\#}$
IGE (80 mg/kg)	$4.25 \pm 0.11^{\#\#}$
IGE (40 mg/kg)	$4.83 \pm 0.14^{\#\#}$
IGE (20 mg/kg)	$5.00 \pm 0.16^{\#}$

Each group represented the value of virus titers. Virus titers was expressed as mean ± SEM ($n = 6$). $^{**}P < 0.01$ compared to normal control group, $^{\#\#}P < 0.01$, $^{\#}P < 0.05$ compared to infection control group.

expression in mice induced by influenza virus infection was significantly depressed by IGE treatment in a dose-dependent manner.

Next, to determine whether the proton channel activity of M2 protein was inhibited by IGE, we further examined the relative changes in endosomal pH using a fluorescent dye, SNARF-1, whose fluorescent properties change in response to changes in intracellular pH (pHi). In more acidic solutions, SNARF-1 fluoresces with an emission peak at around 580 nm, while in more basic solutions the emission peak rises to 640 nm. By comparing the ratios of 640 nm/580 nm emissions, we were able to determine the changes in relative pH. Lower 640/580 nm ratios correlate with a more lower pH.[40]

As shown in Figure 4(a, b) and Supplementary Table 1, the 640/580 nm ratios in the cytoplasm of MDCK cells decreased significantly at 0.5, 1, and 1.5 h post-infection, indicating the declining pHi of the endosome triggered by influenza virus. Moreover during the 1.5 h of influenza infection, pHi reached a minimum at 1 h. Amantadine was used as a positive control, and IGE increased pHi significantly at the concentrations of 25 and 12.5 mg/mL 0.5 or 1 h post-infection, respectively, which demonstrates that endosomal acidification can be prevented by IGE in the early step of influenza virus replication.

Effect of IGE on Ca^{2+} influx

Previous reports suggest that several types of virus infections trigger an extracellular Ca^{2+} influx that leads to cell apoptosis by inducing mitochondrial dysfunction. To explore the Ca^{2+} dynamics in MDCK infected with influenza virus and the effect of IGE on it, cells were stained with fluo-3 AM dye as an indicator of Ca^{2+} in the cytosol ($[Ca^{2+}]_i$). As shown in Figure 5(a, b) and Supplementary Table 2, MDCK infected with influenza virus showed a significant increase in $[Ca^{2+}]_i$ at 0.5,1 and 1.5 h post-infection. In particular, during the 1.5 h of influenza infection, $[Ca^{2+}]_i$ levels reached maximum at 1 h. IGE treatment inhibited elevation of $[Ca^{2+}]_i$ significantly at the concentration of 25 and 12.5 mg/mL 0.5 h or 1 h post-infection, respectively, which indicates that Ca^{2+} influx can be prevented by IGE in the early step of influenza virus replication. At 24 h post-infection, the elevated $[Ca^{2+}]_i$ levels were significantly decreased by IGE at the concentrations of 25 and 12.5 mg/mL, which demonstrates that the elevation in $[Ca^{2+}]_i$ during the pathogenic progress of influenza infection can be reduced by IGE.

Inhibitory effect of IGE on influenza-virus-induced apoptosis

To determine whether the apoptosis induced by influenza virus was inhibited by IGE, MDCK cells were distinguished and sub-divided on the basis of a double-labeling for annexin V-FITC and PI and quantitatively analyzed by flow cytometry.[41] Early-apoptotic cells were only stained with Annexin V-FITC whereas late-apoptotic cells were stained with both Annexin V-FITC and PI. As shown in Figure 6(a, b), the proportion of apoptotic cells labeled with Annexin V/PI was increased from $5.81 \pm 0.56\%$ in control cells to $19.31 \pm 1.17\%$ in the virus infection cells, suggesting a more than three-fold increase in apoptotic cells. However, the proportions of apoptotic cells were decreased to $9.09 \pm 0.76\%$, $10.09 \pm 0.51\%$ and $13.95 \pm 0.91\%$, respectively, with IGE treatment (25, 12.5 and 6.25 mg/mL). In addition, the percentage of early-apoptotic cells increased obviously post 24 h infection, while the late-apoptotic cells did not. As shown in Figure 6(c, d), IGE reduced the percentage of early-apoptotic cells at the concentration of 25, 12.5 and 6.25 mg/mL, but showed no apparent effect on the percentage of late-apoptotic cells. These results demonstrate that early apoptosis of MDCK cells induced by influenza virus infection was significantly inhibited by IGE in a dose-dependent manner.

Discussion

TCM has performed well in clinical practice and has shown potential in the therapy of influenza.[25] For the future prevention and control of influenza outbreaks, it will therefore be critical to develop novel agents from TCM. Our previous study showed that the extract of Gardeniae possessed antiviral activity against influenza virus based on a mice pneumonia model *in vivo*.[30,32] The present study was designed to demonstrate the anti-influenza activity of iridoid glycoside extracted from *Fructus Gardeniae* (IGE), and to investigate the mechanism of antiviral action. The results demonstrate that IGE possesses potent antiviral features against

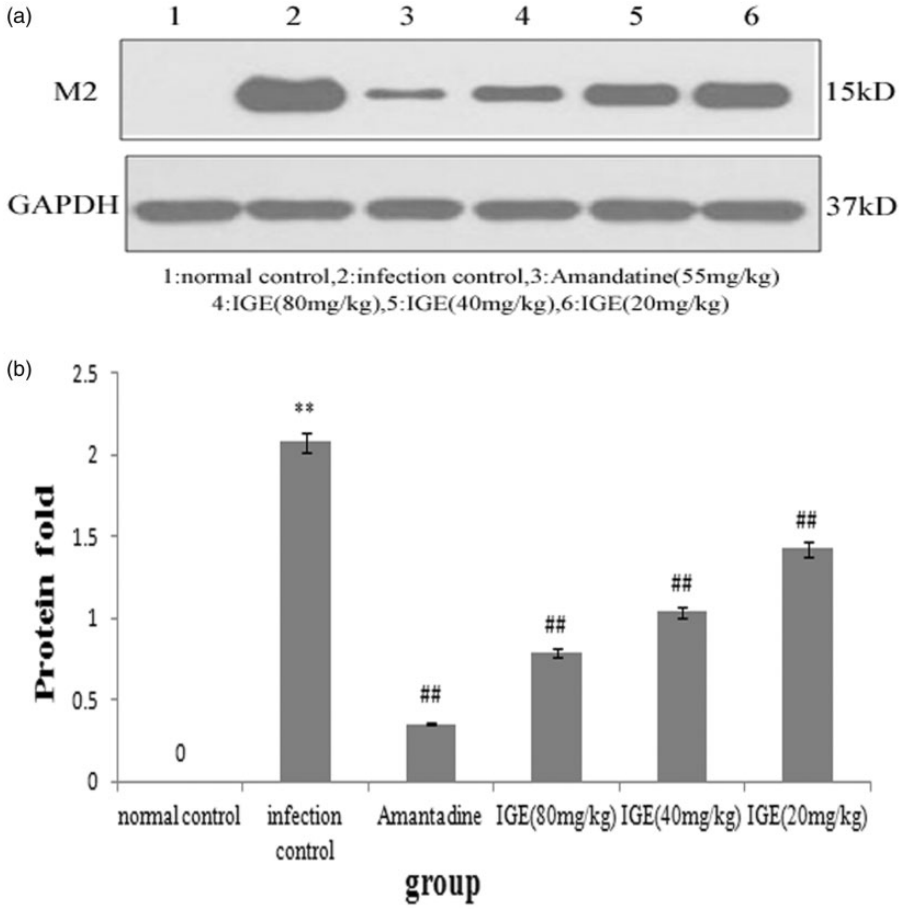

Figure 3 Effect of IGE on M2 protein expression in lung tissues of mice infected by influenza A virus. Values were expressed as the mean ± SEM. (a) IGE inhibited M2 protein expression measured by Western blotting analysis. (b) The relative protein level of M2 normalized by GAPDH ($n = 4$). $^{**}P < 0.01$ compared to normal control group, $^{\#\#}P < 0.01$ compared to infection control group

influenza A virus at non-cytotoxic concentrations *in vitro*. The occurrence of CPEs induced by H1N1 and H3N2 subtypes of influenza A virus in MDCK cells was strongly inhibited by IGE at the concentrations of 25, 12.5 and 6.25 mg/mL, and then, according to the RT-PCR assay, the replication of influenza virus A/FM1/47 in MDCK cells was markedly inhibited by IGE. Moreover, *in vivo* IGE exhibited an inhibitory effect on PI and virus titers in lungs in a dose-dependent manner, indicating that IGE protected the lung from influenza A virus-induced injury. This study therefore provides direct evidence that IGE may represent a potential therapeutic agent for influenza.

The influenza A virus genome is contained on eight single RNA strands that code for 11 proteins. The small coding capacity demands that the virus utilize the host cellular machinery for many aspects of its life cycle.[42] Accordingly, identification of host factors involved in viral replication steps is of great interest to understand the precise mechanisms of the virus life cycle as well as to discover new targets for the development of antiviral compounds.[43] To our knowledge, proton and Ca^{2+} were confirmed to be required for early-stage influenza virus replication as host factors. So we proceeded to investigate the possible mechanisms of IGE anti-influenza virus from these two host factors' related targets and functions.

The incremental acidification of the endosome is essential for the release of the influenza virus genetic material inside an infected cell.[44] Moreover the integral membrane protein M2 of influenza virus forms pH-gated proton channels in the viral lipid envelope to mediate endosomal acidification.[45] In addition, Ca^{2+} plays an important role in almost every step of the virus replication cycle. The fusion between the viral envelop and the susceptible cell plasma membrane leads to an increase of free cytosolic Ca^{2+} ($[Ca^{2+}]CYT$) due to increased plasma membrane permeability and altered membrane permeability of internal Ca^{2+} stores, such as endoplasmic reticulum (ER) and mitochondria.[46] Previous studies have demonstrated that this alteration in the concentration of Ca^{2+} inside the cells infected by influenza virus is essential for activating the apoptotic signaling pathway.[23,47] Therefore, extracellular Ca^{2+} influx and elevations in $[Ca^{2+}]i$ may be important precursors to the pathophysiology caused by influenza infection.

IGE has exhibited a significant inhibitory effect against influenza A virus H1N1 and H3N2 subtypes, so in order to investigate the mechanisms of IGE anti-influenza at the early-stage of virus replication, we detected the effect of IGE on intracellular acidification and extracellular Ca^{2+} influx induced by the influenza virus and the related

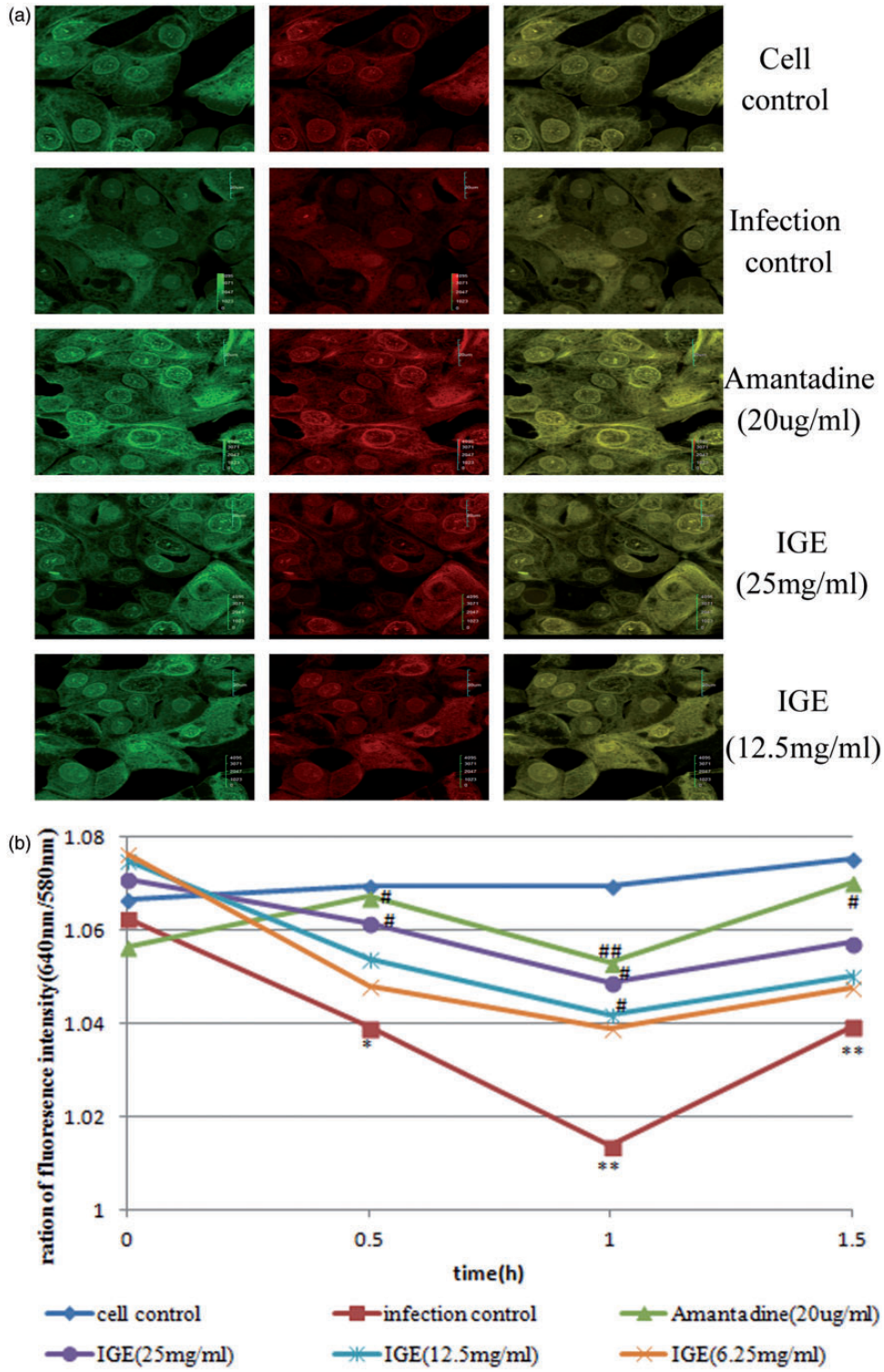

Figure 4 Effect of IGE on pHi in MDCK cells infected with influenza virus. Values were expressed as the mean ratios of 640 nm/580 nm SNARF-1 emission with 5 samples in each group. In each sample 8 randomly selected fields were analyzed. (a) Confocal images of MDCK cells loaded with SNARF-1 probe at 1 h post-infection. Green images represent fluorescence images taken at emission of 580 nm, red images represent fluorescence images taken at emission of 640 nm, yellow image represent merged image of fluorescence images at 580 and 640 nm. (b) The relative pHi was represented by 640/580 nm ratio ($n = 5$). $^{**}P < 0.01$, $^{*}P < 0.05$ compared to cell control group, $^{\#}P < 0.05$ compared to infection control group. (A color version of this figure is available in the online journal.)

pathogenic mechanisms. Our study showed that IGE suppressed the expression of M2 protein in mice lungs in a dose-dependent manner, and enhanced the declining pHi induced by influenza A virus in MDCK cells at 0.5 and 1 h post-infection. Of greater interest in the present study is that at 0.5 and 1 h post-infection, the elevated $[Ca^{2+}]_i$ levels, and cells induced by influenza A virus, were significantly reduced by IGE at the concentration of 25 and

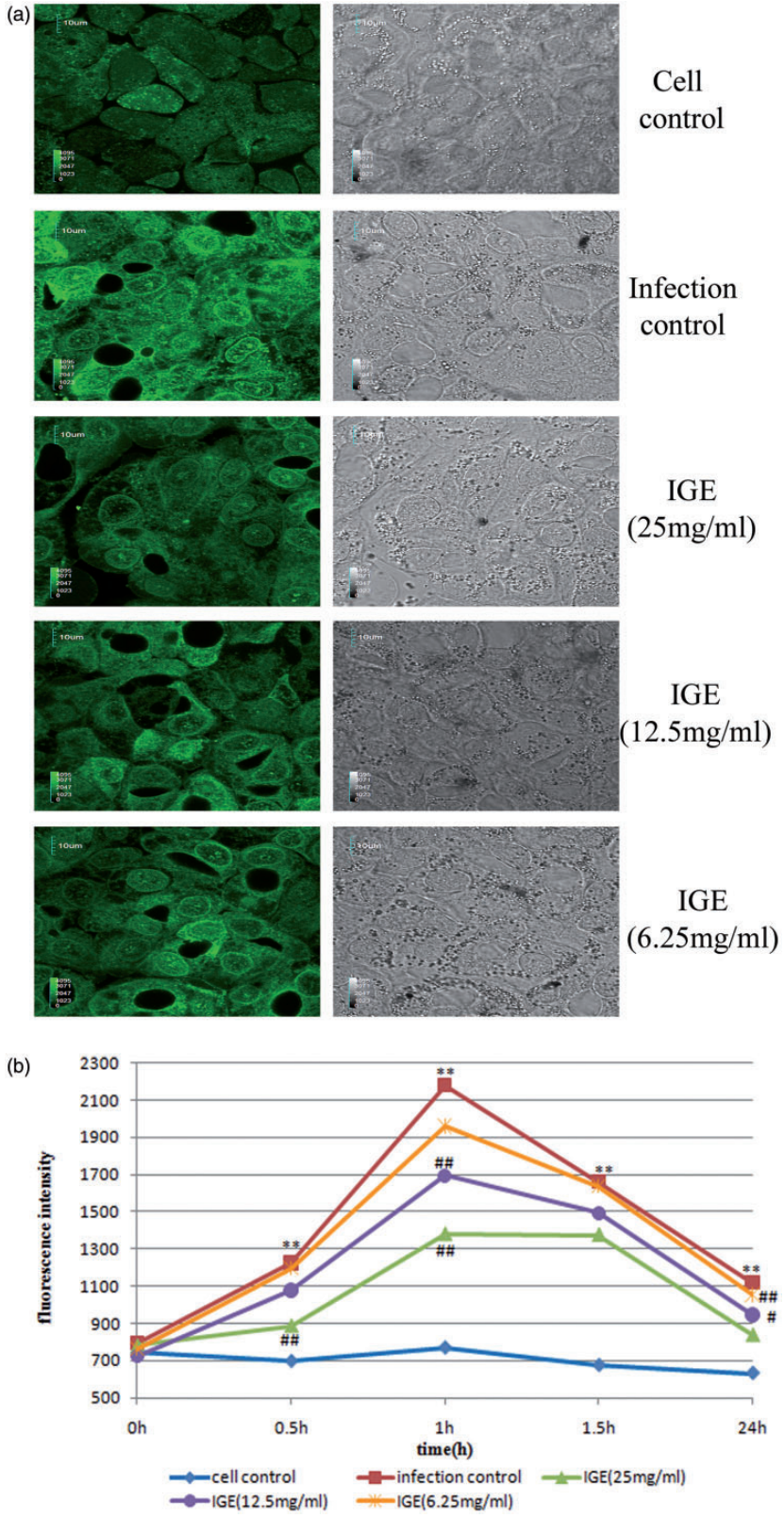

Figure 5 Effect of IGE on $[Ca^{2+}]_i$ levels in MDCK cells infected with influenza virus. Values were expressed as the mean fluorescence intensity of fluo-3 with 4 samples in each group. In each sample 8 randomly selected fields were analyzed. (a) Confocal images of MDCK cells stained with fluo-3 probe at 1 h post-infection. Green images represent fluorescence images taken at emission of 530 nm. Grayscale images represent control images of MDCK cells without fluo-3 staining. (b) The concentration of $[Ca^{2+}]_i$ was represented by mean fluorescence intensity ($n = 4$). $^{**}P < 0.01$ compared to cell control group, $^{\#\#}P < 0.01$, $^{\#}P < 0.05$ compared to infection control group. (A color version of this figure is available in the online journal.)

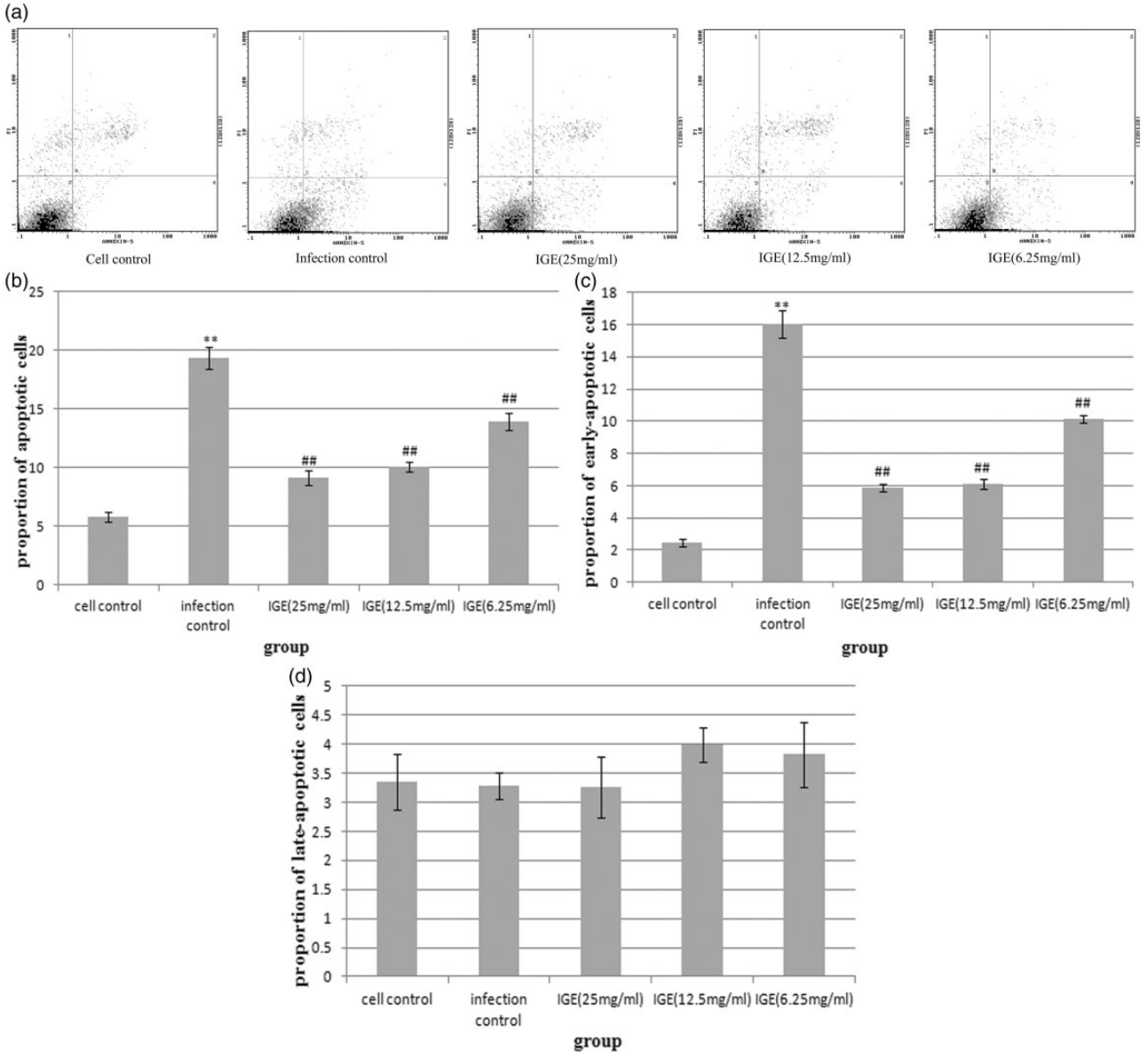

Figure 6 Effect of IGE on apoptosis of MDCK cells infected with influenza virus. Values were expressed as the mean ± SEM. (a) Typical quadrant analysis of Annexin V-FITC/PI flow cytometry of MDCK cells apoptosis. The proportion (%) of cell number is shown in each quadrant. The proportion of viable cells was shown in 3 quadrant ($FITC^-/PI^-$), early apoptotic cells shown in 4 quadrant ($FITC^+/PI^-$), late-apoptotic/necrotic cells shown in 2 quadrant ($FITC^+/PI^+$). (b) The proportion of apoptotic cells by quantitative analysis ($n = 6$). $^{**}P < 0.01$ compared to cell control group, $^{\#\#}P < 0.01$ compared to infection control group. (c) The proportion of early-apoptotic cells by quantitative analysis ($n = 6$). $^{**}P < 0.01$ compared to cell control group, $^{\#\#}P < 0.01$ compared to infection control group. (d) The proportion of late-apoptotic cells by quantitative analysis ($n = 6$)

12.5 mg/mL. In addition, at 24 h post-infection, the rates of early-apoptotic cells being induced by influenza A virus were clearly reduced by IGE as well as $[Ca^{2+}]i$, in a dose-dependent manner. However, there was no apparent effect of virus infection and IGE treatment on the rates of late-apoptotic cells.

The results suggest that IGE strongly inhibits the endosomal acidification which is mediated by M2 proton channel of influenza virus A/FM/1/47 and Ca^{2+} influx which may be related to pathogenic progress of influenza virus A/FM/1/47 infection. However, further investigations into the effect of IGE on the relationship of Ca^{2+} imbalance and pathogenesis of influenza virus need to be verified.

It was reported that in the early steps of HSV-1 replication, Gardenia extract had an effect on the cellular machinery, including membrane fluidity, membrane potential and ATPase.[48] In this study, we investigated the anti-influenza mechanisms of IGE against influenza in early-stage virus replication at 0.5, 1 and 1.5 h post-infection. The intracellular concentrations of both H^+ and Ca^{2+} in MDCK cells reached their peak at 1 h post-infection, but IGE reversed the elevation at 0.5 and 1 h post-infection. This suggests that IGE acts on pivotal ions at an early stage in the replication cycle of influenza virus. In addition, IGE suppressed the expression of M2 protein which mediated the endosomal acidification induced by influenza virus. Virus-induced

apoptosis is a complex and important aspect of the pathogenesis of viral infection.[49,50] Our results suggest that IGE could decrease the intracellular concentration of calcium and early apoptosis induced by influenza virus. Further investigations are required to determine the pathways involved in the inhibition effect of IGE on the replication, and on the pathological progress of influenza virus via intracellular acidification and Ca^{2+} influx.

In conclusion, our study shows that IGE has antiviral effects both in a murine model of viral pneumonia, and also in MDCK cells experiencing a CPE induced by influenza virus. These antiviral effects might be related to the inhibition of intracellular acidification and Ca^{2+} influx during fusion and the uncoating of the influenza replication cycle. These findings suggest that IGE might be applicable to the treatment of patients suffering from influenza. Further studies should be focused on discovering the effect of IGE on the virus–host interaction and in elucidating the molecular target and related signal pathways.

Author contributions: SG and XC designed the study; SG, YG, YJ and XT performed the experiment; SG and XT analyzed and interpreted the data; SG wrote the manuscript.

ACKNOWLEDGMENTS

The project was funded by the following grants: China Postdoctoral Science Foundation (No. 2012M520557), National Natural Science Foundation of China (No. 81303290), Beijing Natural Science Foundation of China (No. 7132141), China Basic Research Projects of China Academy of Chinese Medical Sciences (No. ZZ20090103, 2011ZDXK-03).

REFERENCES

1. Tao QWaYJ, Ed. *Influenza: molecular virology.* Norfolk, UK: Caister Academic Press, 2010
2. Basler CF. Influenza viruses: basic biology and potential drug targets. *Infect Disord Drug Targets* 2007;**7**:282–93
3. Peiris JS, de Jong MD, Guan Y. Avian influenza virus (H5N1): a threat to human health. *Clin Microbiol Rev* 2007;**20**:243–67
4. Taubenberger JK, Reid AH, Lourens RM, Wang R, Jin G, Fanning TG. Characterization of the 1918 influenza virus polymerase genes. *Nature* 2005;**437**:889–93
5. Taubenberger JK, Morens DM. 1918 Influenza: the mother of all pandemics. *Emerg Infect Dis* 2006;**12**:15–22
6. Horimoto T, Kawaoka Y. Influenza: lessons from past pandemics, warnings from current incidents. *Nat Rev Microbiol* 2005;**3**:591–600
7. Beigel JH, Farrar J, Han AM, Hayden FG, Hyer R, de Jong MD, Lochindarat S, Nguyen TK, Nguyen TH, Tran TH, Nicoll A, Touch S, Yuen KY. Avian influenza A (H5N1) infection in humans. *N Engl J Med* 2005;**353**:1374–85
8. Li KS, Guan Y, Wang J, Smith GJ, Xu KM, Duan L, Rahardjo AP, Puthavathana P, Buranathai C, Nguyen TD, Estoepangestie AT, Chaisingh A, Auewarakul P, Long HT, Hanh NT, Webby RJ, Poon LL, Chen H, Shortridge KF, Yuen KY, Webster RG, Peiris JS. Genesis of a highly pathogenic and potentially pandemic H5N1 influenza virus in eastern Asia. *Nature* 2004;**430**:209–13
9. Neumann G, Noda T, Kawaoka Y. Emergence and pandemic potential of swine-origin H1N1 influenza virus. *Nature* 2009;**459**:931–9
10. (WHO) WHO. Disease outbreak news: pandemic (H1N1) 2009-update 110. Geneva, 2009
11. (WHO) WHO. Global alert and response (GAR): human infection with influenza A (H7N9) virus in China. Geneva, 2013
12. (CDC) CfDCaP. Morbidity and mortality weekly report (MMWR): emergence of Avian influenza A (H7N9) virus causing severe human illness-China, February–April 2013
13. Ibricevic A, Pekosz A, Walter MJ, Newby C, Battaile JT, Brown EG, Holtzman MJ, Brody SL. Influenza virus receptor specificity and cell tropism in mouse and human airway epithelial cells. *J Virol* 2006;**80**:7469–80
14. Ma C, Polishchuk AL, Ohigashi Y, Stouffer AL, Schon A, Magavern E, Jing X, Lear JD, Freire E, Lamb RA, DeGrado WF, Pinto LH. Identification of the functional core of the influenza A virus A/M2 proton-selective ion channel. *Proc Natl Acad Sci U S A* 2009;**106**:12283–8
15. Fontana J, Steven AC. At low pH, influenza virus matrix protein M1 undergoes a conformational change prior to dissociating from the membrane. *J Virol* 2013;**87**:5621–8
16. Ciampor F, Thompson CA, Grambas S, Hay AJ. Regulation of pH by the M2 protein of influenza A viruses. *Virus Res* 1992;**22**:247–58
17. Adamson AL, Chohan K, Swenson J, LaJeunesse D. A Drosophila model for genetic analysis of influenza viral/host interactions. *Genetics* 2011;**189**:495–506
18. Giorgi C, Romagnoli A, Pinton P, Rizzuto R. Ca2+ signaling, mitochondria and cell death. *Curr Mol Med* 2008;**8**:119–30
19. Hajnoczky G, Davies E, Madesh M. Calcium signaling and apoptosis. *Biochem Biophys Res Commun* 2003;**304**:445–54
20. Saggioro D, Silic-Benussi M, Biasiotto R, D'Agostino DM, Ciminale V. Control of cell death pathways by HTLV-1 proteins. *Front Biosci (Landmark Ed)* 2009;**14**:3338–51
21. Benali-Furet NL, Chami M, Houel L, De Giorgi F, Vernejoul F, Lagorce D, Buscail L, Bartenschlager R, Ichas F, Rizzuto R, Paterlini-Brechot P. Hepatitis C virus core triggers apoptosis in liver cells by inducing ER stress and ER calcium depletion. *Oncogene* 2005;**24**:4921–33
22. Bonavia R, Bajetto A, Barbero S, Albini A, Noonan DM, Schettini G. HIV-1 Tat causes apoptotic death and calcium homeostasis alterations in rat neurons. *Biochem Biophys Res Commun* 2001;**288**:301–8
23. Ueda M, Daidoji T, Du A, Yang CS, Ibrahim MS, Ikuta K, Nakaya T. Highly pathogenic H5N1 avian influenza virus induces extracellular Ca2+ influx, leading to apoptosis in avian cells. *J Virol* 2010;**84**:3068–78
24. Kuwano K. Epithelial cell apoptosis and lung remodeling. *Cell Mol Immunol* 2007;**4**:419–29
25. Wang X, Jia W, Zhao A. Anti-influenza agents from plants and traditional Chinese medicine. *Phytother Res* 2006;**20**:335–41
26. Ge H, Wang YF, Xu J, Gu Q, Liu HB, Xiao PG, Zhou J, Liu Y, Yang Z, Su H. Anti-influenza agents from traditional Chinese medicine. *Nat Prod Rep* 2010;**27**:1758–80
27. Nakayama T, Suzuki S, Kudo H, Sassa S, Nomura M, Sakamoto S. Effects of three Chinese herbal medicines on plasma and liver lipids in mice fed a high-fat diet. *J Ethnopharmacol* 2007;**109**:236–40
28. Hong YJ, Yang KS. Anti-inflammatory activities of crocetin derivatives from processed Gardenia jasminoides. *Arch Pharm Res* 2013;**36**:933–40
29. Ni HY, Zhang ZH, Fu HZ. [Research and development of Fructus Gardeniae]. *Zhongguo Zhong Yao Za Zhi* 2006;**31**:538–41
30. Wang YZ, Cui XL, Gao YJ, Guo SS, Wang XK, Huang Y, Zhao Y, Gong WF. [Antivirus effects of extract from gardenia]. *Zhongguo Zhong Yao Za Zhi* 2006;**31**:1176–8
31. Guo SS, Huang Y, Zhao Y, Gao YJ, Gong WF, Cui XL. [Effect of extracted ZG from gardenia on Hep-2 cell membrane post infected with parainfluenza virus type 1 (PIV-1)]. *Bing Du Xue Bao* 2007;**23**:384–8
32. Yang Q, Wu B, Shi Y, Du X, Fan M, Sun Z, Cui X, Huang C. Bioactivity-guided fractionation and analysis of compounds with anti-influenza virus activity from Gardenia jasminoides Ellis. *Arch Pharm Res* 2012;**35**:9–17
33. Li HB, Yu Y, Wang ZZ, Dai Y, Gao H, Xiao W, Yao XS. Iridoid and bisiridoid glucosides from the fruit of Gardenia jasminoides. *Fitoterapia* 2013;**88C**:7–11
34. Quanjun Yang MF, Bin Wu, Zhaolin Sun, Xiaolan Cui, Xiaowei Du, Chenggang Huang. Quality assessment for fructus Gardeniae by multicomponent quantification, chromatographic fingerprint and related chemometric analysis. *J Med Plants Res* 2011;**5**:4126–37

35. Hierholzer JC, Killington RA. *Virus isolation and quantitation*. London: Academic Press, 1996
36. Mosmann T. Rapid colorimetric assay for cellular growth and survival: application to proliferation and cytotoxicity assays. *J Immunol Methods* 1983;**65**:55–63
37. Han J, Burgess K. Fluorescent indicators for intracellular pH. *Chem Rev* 2010;**110**:2709–28
38. Loughrey CM, MacEachern KE, Cooper J, Smith GL. Measurement of the dissociation constant of Fluo-3 for Ca2+ in isolated rabbit cardiomyocytes using Ca2+ wave characteristics. *Cell Calcium* 2003;**34**:1–9
39. Kolocouris N, Zoidis G, Foscolos GB, Fytas G, Prathalingham SR, Kelly JM, Naesens L, De Clercq E. Design and synthesis of bioactive adamantane spiro heterocycles. *Bioorg Med Chem Lett* 2007;**17**:4358–62
40. Vaughan-Jones RD, Peercy BE, Keener JP, Spitzer KW. Intrinsic H(+) ion mobility in the rabbit ventricular myocyte. *J Physiol* 2002;**541**:139–58
41. Chen S, Cheng AC, Wang MS, Peng X. Detection of apoptosis induced by new type gosling viral enteritis virus in vitro through fluorescein annexin V-FITC/PI double labeling. *World J Gastroenterol* 2008;**14**:2174–8
42. Konig R, Stertz S, Zhou Y, Inoue A, Hoffmann HH, Bhattacharyya S, Alamares JG, Tscherne DM, Ortigoza MB, Liang Y, Gao Q, Andrews SE, Bandyopadhyay S, De Jesus P, Tu BP, Pache L, Shih C, Orth A, Bonamy G, Miraglia L, Ideker T, Garcia-Sastre A, Young JA, Palese P, Shaw ML, Chanda SK. Human host factors required for influenza virus replication. *Nature* 2010;**463**:813–7
43. Watanabe T, Watanabe S, Kawaoka Y. Cellular networks involved in the influenza virus life cycle. *Cell Host Microbe* 2010;**7**:427–39
44. Tran L, Choi SB, Al-Najjar BO, Yusuf M, Wahab HA, Le L. Discovery of potential M2 channel inhibitors based on the amantadine scaffold via virtual screening and pharmacophore modeling. *Molecules* 2011;**16**:10227–55
45. Du QS, Huang RB, Wang SQ, Chou KC. Designing inhibitors of M2 proton channel against H1N1 swine influenza virus. *PLoS One* 2010;**5**:e9388
46. Zhou Y, Frey TK, Yang JJ. Viral calciomics: interplays between Ca2+ and virus. *Cell Calcium* 2009;**46**:1–17
47. Daidoji T, Koma T, Du A, Yang CS, Ueda M, Ikuta K, Nakaya T. H5N1 avian influenza virus induces apoptotic cell death in mammalian airway epithelial cells. *J Virol* 2008;**82**:11294–307
48. Wang Xiukun GS, Huang Yang, Zhao Ye, Gao Yingjie, Gong Wenfeng, Cui Xiaolan. Effect of Gardenia extract ZG on the membrane fluidity of Hep-2 cell infected by herpes simplex virus type1. *Chin J Microbiol Immunol* 2006;**26**:1005–8
49. Tham KM, Moon CD. Apoptosis in cell cultures induced by infectious bursal disease virus following in vitro infection. *Avian Dis* 1996;**40**:109–13
50. Koyama AH, Fukumori T, Fujita M, Irie H, Adachi A. Physiological significance of apoptosis in animal virus infection. *Microbes Infect* 2000;**2**:1111–7

(Received August 13, 2013, Accepted January 26, 2014)